Cyclin B–Cdk1 inhibits protein phosphatase PP2A-B55 via a Greatwall kinase–independent mechanism

Eiichi Okumura,[1] Atsushi Morita,[1] Mizuho Wakai,[1] Satoru Mochida,[2] Masatoshi Hara,[1] and Takeo Kishimoto[1,3]

[1]Laboratory of Cell and Developmental Biology, Graduate School of Bioscience, Tokyo Institute of Technology, Yokohama 226-8501, Japan
[2]Priority Organization for Innovation and Excellence, Kumamoto University, Kumamoto 860-0811, Japan
[3]Science and Education Center, Ochanomizu University, Tokyo 112-8610, Japan

Entry into M phase is governed by cyclin B–Cdk1, which undergoes both an initial activation and subsequent autoregulatory activation. A key part of the autoregulatory activation is the cyclin B–Cdk1–dependent inhibition of the protein phosphatase 2A (PP2A)–B55, which antagonizes cyclin B–Cdk1. Greatwall kinase (Gwl) is believed to be essential for the autoregulatory activation because Gwl is activated downstream of cyclin B–Cdk1 to phosphorylate and activate α-endosulfine (Ensa)/Arpp19, an inhibitor of PP2A-B55. However, cyclin B–Cdk1 becomes fully activated in some conditions lacking Gwl, yet how this is accomplished remains unclear. We show here that cyclin B–Cdk1 can directly phosphorylate Arpp19 on a different conserved site, resulting in inhibition of PP2A-B55. Importantly, this novel bypass is sufficient for cyclin B–Cdk1 autoregulatory activation. Gwl-dependent phosphorylation of Arpp19 is nonetheless necessary for downstream mitotic progression because chromosomes fail to segregate properly in the absence of Gwl. Such a biphasic regulation of Arpp19 results in different levels of PP2A-B55 inhibition and hence might govern its different cellular roles.

Introduction

The kinase cyclin B–Cdc2/Cdk1 is a universal regulator of M phase (Nurse, 1990). After the cyclin B–Cdk1 complex is first formed, its activity is regulated by the balance of activity between Wee1/Myt1 kinase that phosphorylates Cdk1 for inhibition and Cdc25 phosphatase that dephosphorylates the Wee1/Myt1 sites for activation (Lew and Kornbluth, 1996). At the G2/M phase border, the cyclin B–Cdk1 complex is already present but is kept inactive because the balance is inclined to the inhibitory phosphorylation. At the initial onset of M phase, the balance is tipped to initially activate a small population of cyclin B–Cdk1. Subsequently, a much larger population of cyclin B–Cdk1 becomes activated through an autoregulatory loop in which active cyclin B–Cdk1 further inactivates Wee1/Myt1 and activates Cdc25 (Lew and Kornbluth, 1996; Ferrell et al., 2009; Lindqvist et al., 2009). An additional core element of the autoregulatory loop is the cyclin B–Cdk1–dependent inhibition of protein phosphatase 2A (PP2A)–B55, the phosphatase that antagonizes the effects of cyclin B–Cdk1 on Wee1/Myt1 and Cdc25 (Mochida and Hunt, 2012). In this inhibitory PP2A-B55 pathway, cyclin B–Cdk1 activates Greatwall kinase (Gwl; Yu et al., 2006); Gwl in turn phosphorylates the small protein α-endosulfine (Ensa) and/or its close relative cyclic adenosine monophosphate–regulated phosphoprotein 19 (Arpp19); and then phosphorylated Ensa/Arpp19 suppresses PP2A-B55 activity (Zhao et al., 2008; Castilho et al., 2009; Mochida et al., 2009, 2010; Vigneron et al., 2009; Gharbi-Ayachi et al., 2010; Lorca et al., 2010; Rangone et al., 2011; Kim et al., 2012).

However, inconsistencies exist in the literature as to whether Gwl is always required for cyclin B–Cdk1 activation. Gwl is essential for cyclin B–Cdk1 activation or entry into M phase in cycling extracts from frog eggs (Yu et al., 2006) and in many types of fruit fly cells (Yu et al., 2004). In contrast, Gwl is not always required for human cell proliferation because some cells strongly depleted of Gwl/MASTL are delayed in G2 phase but finally enter into M phase (Burgess et al., 2010; Voets and

Correspondence to Takeo Kishimoto: tkishimo@bio.titech.ac.jp or kishimoto.takeo@ocha.ac.jp

M. Hara's present address is Whitehead Institute and Dept. of Biology, Massachusetts Institute of Technology, Cambridge, MA 02142.

Abbreviations used in this paper: Arpp19, cyclic adenosine monophosphate–regulated phosphoprotein 19; Ensa, α-endosulfine; GVBD, germinal vesicle breakdown; Gwl, Greatwall kinase; 1-MeAde, 1-methyladenine; PP2A, protein phosphatase 2A.

The Rockefeller University Press $30.00
J. Cell Biol. Vol. 204 No. 6 881–889
www.jcb.org/cgi/doi/10.1083/jcb.201307160

Wolthuis, 2010). Even more strikingly, Gwl is absolutely unnecessary in meiosis I of starfish oocytes (see following paragraph; Hara et al., 2012); and the nematode *Caenorhabditis elegans* has no obvious Gwl kinase (Kim et al., 2012). It is thus possible that other pathways may act to shut down the activity of PP2A-B55 during the autoregulatory activation of cyclin B–Cdk1.

Immature oocytes generally arrest their cell cycle at the G2/M phase border of the first meiosis (Kishimoto, 2003). The meiotic G2/M phase transition in starfish oocytes is induced by the extracellular action of the maturation-inducing hormone 1-methyladenine (1-MeAde; Kanatani et al., 1969), which results in the intracellular activation of cyclin B–Cdk1 with no requirement for new protein synthesis (Kishimoto, 2011). In starfish oocytes (Hara et al., 2012) as well as in fruit fly (Yu et al., 2004) and human (Burgess et al., 2010; Voets and Wolthuis, 2010) somatic cells, Gwl is exclusively present in the nucleus (germinal vesicle) and is activated downstream of cyclin B–Cdk1. When Gwl activity is depleted either by prior enucleation from immature oocytes (Kishimoto et al., 1981) or by injection of neutralizing anti-Gwl antibody that can inhibit Gwl activity (Hara et al., 2012), cyclin B–Cdk1 is activated nearly normally (Hara et al., 2012). It is thus intriguing to ask how the autoregulatory activation of cyclin B–Cdk1 is accomplished in the absence of Gwl. We show here that cyclin B–Cdk1 directly phosphorylates Arpp19 on a different conserved site to inhibit PP2A-B55, resulting in the autoactivation of cyclin B–Cdk1 without Gwl.

Results and discussion

Arpp19 is required for cyclin B–Cdk1 activation regardless of the presence or absence of Gwl

PP2A-B55 is known to be largely cytoplasmic in both fruit fly (Mayer-Jaekel et al., 1994) and mammalian cells (Santos et al., 2012; Álvarez-Fernández et al., 2013). It is thus conceivable that inhibition of PP2A-B55 is accomplished after 1-MeAde addition in enucleated (i.e., Gwl-depleted) starfish oocytes as well because inhibition of PP2A-B55 is thought to be required for full activation of cyclin B–Cdk1. Consistently, phosphorylated Fizzy-Ser50 (Fizzy-pSer50; see Materials and methods), a major phosphatase of which is PP2A-B55 (Mochida et al., 2009), was dephosphorylated in enucleated immature oocytes, whereas it remained at the phosphorylated state after 1-MeAde treatment (Fig. 1 A).

We then examined whether Ensa/Arpp19 is required for activation of cyclin B–Cdk1 in enucleated oocytes. For this purpose, a cDNA of starfish homologue of Ensa/Arpp19 was first isolated (Fig. S1). Although only a single homologue of Ensa/Arpp19 was found, this is a commonly encountered phenomenon in starfish (Abe et al., 2010). In fact, database searches revealed that there is also a single homologue of Ensa/Arpp19 in the *C. elegans*, fruit fly, sea urchin, and amphioxus genomes, suggesting that invertebrates have a only one homologue of Ensa/Arpp19. Because the starfish homologue was more similar to Arpp19 than Ensa, it is hereafter called starfish Arpp19. A putative phosphorylation site targeted by Gwl is conserved at Ser106 in starfish Arpp19.

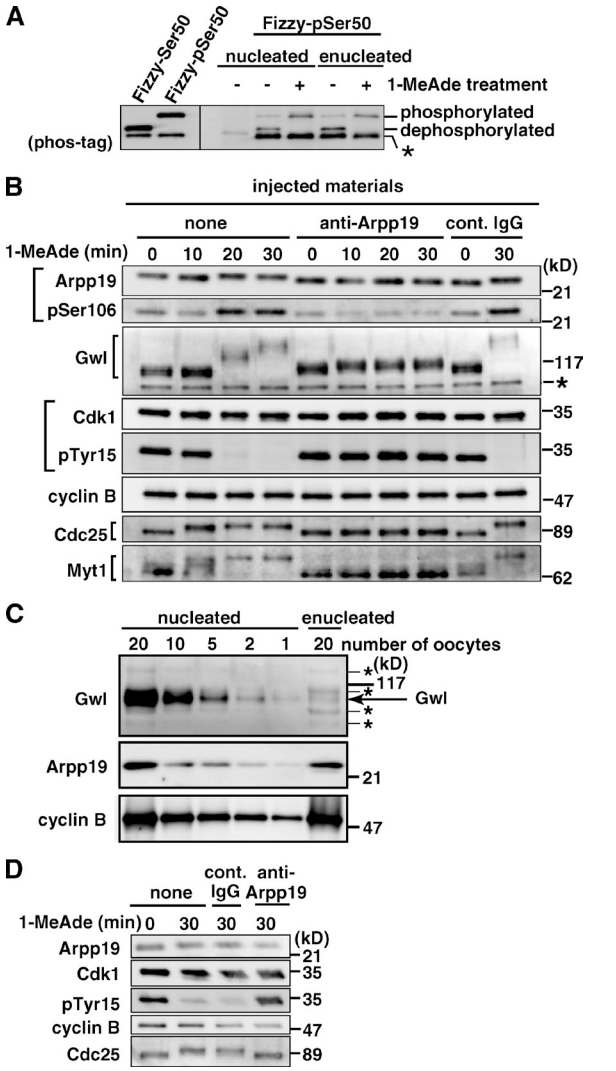

Figure 1. **Arpp19 is required for cyclin B–Cdk1 activation regardless of the presence or absence of nucleus.** (A) PP2A-B55 activity is possibly suppressed after 1-MeAde addition in enucleated as well as nucleated oocytes. Fizzy-pSer50 was injected into nucleated or enucleated oocytes at G2 phase (1-MeAde untreated, −) or M phase (1-MeAde treated, +; at a time equivalent to GVBD). 15 min later, phosphorylation states of Fizzy-Ser50 were analyzed by Western blot. Asterisk, nonspecific band. (B) Anti-Arpp19 antibody inhibits cyclin B–Cdk1 activation in nucleated oocytes. Immature oocytes were uninjected (none) or injected with either anti-Arpp19 antibody or control IgG, and then treated with 1-MeAde. After collection of oocytes at the indicated times, immunoblots were performed with the indicated antibodies. Numbers on the right indicate molecular mass. (C) Arpp19 is largely cytoplasmic. Protein amounts in immature oocytes were compared with immunoblots. Gwl is a nuclear marker and cyclin B is a cytoplasmic marker. (D) Anti-Arpp19 antibody inhibits cyclin B–Cdk1 activation also in enucleated oocytes. After enucleation (which removes Gwl), oocytes were injected and treated as in B. Note that even after 1-MeAde addition, phospho-Tyr15 in Cdk1 (pTyr15) remained detectable and Cdc25 remained inactive in anti-Arpp19 antibody-injected nucleated (B) and enucleated (D) oocytes. Brightness, contrast, and gamma settings were adjusted in the image presentation.

To characterize Arpp19 in starfish oocytes, we raised in rabbits two types of antibodies against starfish Arpp19: anti–full-length Arpp19 (anti-Arpp19) and anti–phospho-Ser106 of Arpp19 (anti-pSer106) antibodies (Fig. S2, A and B). Arpp19 protein was detectable in immature oocytes (Fig. 1 B), a major fraction of which localized to the cytoplasm (Fig. 1 C). During

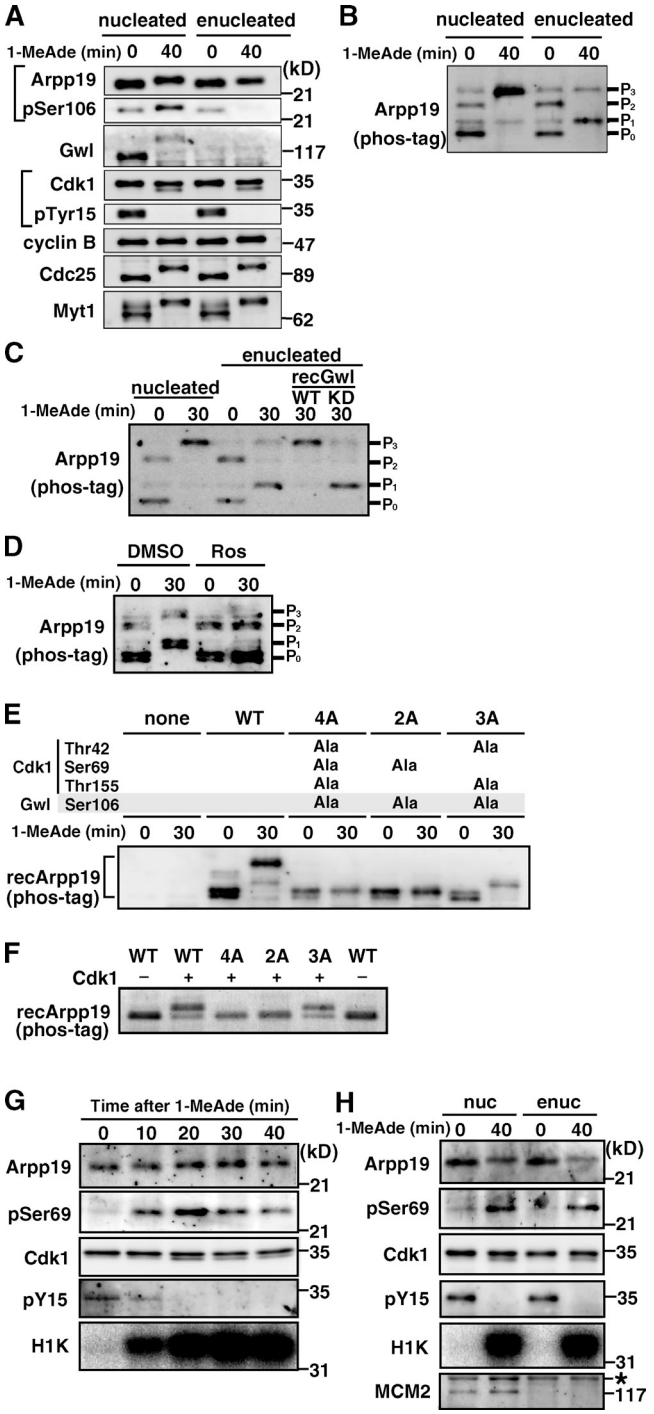

Figure 2. **Arpp19 is phosphorylated on Ser69 by cyclin B–Cdk1 regardless of the presence or absence of Gwl.** (A and B) Arpp19 becomes phosphorylated even in enucleated oocytes after 1-MeAde addition. Nucleated or enucleated oocytes were treated with 1-MeAde, and 40 min later (equivalent to metaphase of meiosis I) conventional (A) and phos-tag (B) SDS-PAGE followed by anti-Arpp19 immunoblots were performed. Entry into M phase was confirmed by loss of pTyr15 in Cdk1. (C) Gwl restores enucleation effects on the phosphorylation pattern of Arpp19. Enucleated immature oocytes were uninjected or injected with recombinant Gwl (recGwl; inactive, WT; control kinase-dead, KD) and then treated with 1-MeAde. Phos-tag analysis as in B was performed in C–F. (D) Inhibition of Cdk1 prevents Arpp19 phosphorylation in enucleated oocytes. Enucleated oocytes were treated with 1-MeAde in the presence of the Cdk inhibitor roscovitine (20 µM; Ros) or control DMSO. (E) Arpp19 becomes phosphorylated not only on the Gwl site, Ser106, but also on a possible Cdk1 site, Ser69, after entry into M phase in nucleated oocytes. Nucleated immature oocytes were injected with wild type (WT) or each mutant of Arpp19 proteins (4A [T42A, S69A, S106A, and T155A], 2A [S69A and S106A], and 3A [T42A, S106A, and T155A]), and then treated with 1-MeAde. The 3A mutant, which retains Ser69, showed the band upshift. (F) Cyclin B–Cdk1 directly phosphorylates Arpp19 on Ser69 in vitro. Each of wild-type Arpp19 and the mutant proteins described in E was mixed with purified cyclin B–Cdk1. Wild type and the 3A mutant, both of which retain Ser69, showed the band upshift. (G and H) Arpp19 is phosphorylated on Ser69 in vivo after entry into M phase both in nucleated and enucleated oocytes. Nucleated (G) or enucleated (H) oocytes were treated with 1-MeAde, and oocyte extracts were prepared at the indicated times. Anti-Arpp19 immunoprecipitates were analyzed with anti-pSer69 antibody. Entry into M phase was confirmed by loss of pTyr15 in Cdk1 and by histone H1 kinase (H1K) activation. Enucleation was confirmed by loss of MCM2, a nuclear protein marker (H). Brightness, contrast, and gamma settings were adjusted in the image presentation.

the meiotic G2/M phase transition, protein levels of Arpp19 remained constant, whereas its mobility on SDS-PAGE became slightly retarded. The levels of Ser106 phosphorylation greatly increased in parallel with activation of both cyclin B–Cdk1 and Gwl, which were indicated by disappearance of phospho-Tyr15 on Cdk1 and by hyperphosphorylation of Gwl, respectively (Fig. 1 B, none).

When nucleated immature oocytes were injected with anti-Arpp19 antibody and then treated with 1-MeAde, no germinal vesicle breakdown (GVBD) was observed. Consistently, cyclin B–Cdk1 failed to become activated and no increase occurred in the levels of Arpp19-Ser106 phosphorylation (Fig. 1 B, anti-Arpp19). These observations support the ideas that the anti-Arpp19 antibody suppresses the effect of endogenous Arpp19 and that Arpp19 is necessary for activation of cyclin B–Cdk1 in nucleated oocytes. In enucleated immature oocytes as well, no activation of cyclin B–Cdk1 was observed when they were injected with the neutralizing anti-Arpp19 antibody and then treated with 1-MeAde (Fig. 1 D). Arpp19 is thus required for cyclin B–Cdk1 activation even in the absence of Gwl.

Arpp19 is phosphorylated on Ser69 by cyclin B–Cdk1 in vitro and in vivo

How can Arpp19 be involved in cyclin B–Cdk1 activation if Gwl is not present? To address this, we first examined more closely the behavior of Arpp19 in enucleated, Gwl-free oocytes (Fig. 2 A). Although no phosphorylation was detectable on Ser106 of Arpp19 when cyclin B–Cdk1 became activated after 1-MeAde addition to enucleated oocytes, a slight shift-up in Arpp19's electrophoretic mobility nevertheless occurred. Changes in the phosphorylation pattern of Arpp19 before and after cyclin B–Cdk1 activation in enucleated oocytes were even clearer using phos-tag SDS-PAGE (Fig. 2 B, particularly the P_1 band). When recombinant Gwl was added back to enucleated oocytes, the P_1 band disappeared, whereas the P_3 band appeared (Fig. 2 C), supporting that the major effect of enucleation is removal of Gwl. Arpp19 is thus most likely phosphorylated in enucleated oocytes by some mitotic kinase other than Gwl.

Ensa/Arpp19 has been reported to be phosphorylated not only by Gwl but also by cyclin B–Cdk1 in M phase, although the role for cyclin B–Cdk1–dependent phosphorylation remains unknown (Gharbi-Ayachi et al., 2010; Mochida et al., 2010).

Starfish Arpp19 contains three putative sites (Thr42, Ser69, and Thr155) for cyclin B–Cdk1 phosphorylation (Fig. S1). In fact, treatment of enucleated oocytes with the Cdk inhibitor roscovitine mostly prevented phosphorylation of Arpp19 after 1-MeAde addition (Fig. 2 D). We made several nonphosphorylatible mutants of Arpp19 at the three putative Cdk1 sites (Thr42, Ser69, and Thr155) and the conserved Gwl site (Ser106). Injection of wild-type or mutant Arpp19 proteins into nucleated immature oocytes revealed that, after 1-MeAde addition, exogenous Arpp19 was phosphorylated at Ser69 (a Cdk1 site) and Ser106 (the Gwl site) during M phase (Fig. 2 E). Consistently, purified cyclin B–Cdk1 phosphorylated in vitro only the mutant (3A) of Arpp19 containing intact Ser69 but not mutants containing Ser69Ala (Fig. 2 F). Thus, Arpp19 is most likely to be phosphorylated on Ser69 by cyclin B–Cdk1, besides Ser106 phosphorylation by Gwl.

To confirm that endogenous Arpp19 is phosphorylated on Ser69 in M phase, we prepared anti–phospho-Ser69 of Arpp19 antibody (anti-pSer69; Fig. S2, C and D). In nucleated oocytes, phosphorylation on Ser69 of Arpp19 became detectable when cyclin B–Cdk1 was activated after 1-MeAde addition (Fig. 2 G). In enucleated oocytes as well, Arpp19 was phosphorylated on Ser69 in M phase (Fig. 2 H). We concluded that endogenous Arpp19 is phosphorylated on Ser69 directly by cyclin B–Cdk1, regardless of the presence or absence of Gwl.

Arpp19 phosphorylated on Ser69 by cyclin B–Cdk1 inhibits PP2A-B55

We then investigated the effect of anti-Arpp19 antibody on the in vitro phosphorylation of Ser69 on Arpp19 by cyclin B–Cdk1. For this purpose, in vitro phosphorylation of Ser69 on Arpp19 by purified cyclin B–Cdk1 (shown in Fig. 2 F) was first confirmed by anti-pSer69 antibody (Fig. 3 A, left). Further addition of the anti-Arpp19 antibody to the reaction mixture inhibited phosphorylation of Ser69 by cyclin B–Cdk1 (Fig. 3 A, left), whereas the same antibody did not inhibit Gwl-induced phosphorylation of Ser106 on Arpp19 (Fig. 3 A, right). Thus, the in vivo inhibitory effect of anti-Arpp19 antibody on cyclin B–Cdk1 activation (Fig. 1) could be ascribed to prevention of cyclin B–Cdk1 phosphorylation of Ser69 on Arpp19.

How then does the phosphorylation of Arpp19 on Ser69 by cyclin B–Cdk1 contribute to the activation of cyclin B–Cdk1? Because PP2A-B55 was presumably down-regulated during M phase in enucleated, Gwl-deficient oocytes (Fig. 1 A), we examined the in vitro effect of the Arpp19-Ser69 phosphorylation on PP2A-B55 activity. For this purpose, a cDNA of the starfish homologue for the B55 subunit of PP2A was cloned (Fig. S3), an antibody was raised against it (Fig. S2 E), and endogenous protein levels of B55 and Arpp19 in starfish oocytes were determined (Fig. 3 B). Then, under conditions that reflect the endogenous molar ratio (i.e., 1:4) between B55 and Arpp19, the effect of the Arpp19-Ser69 phosphorylation on PP2A-B55 activity was examined in vitro (Fig. 3 C). After addition of unphosphorylated Arpp19 or Arpp19 (wild type or mutant) thiophosphorylated by cyclin B–Cdk1, Gwl, or cyclin B–Cdk1 plus Gwl, the phosphatase activity of recombinant PP2A-A/B55δ/C trimer complex was compared by measuring the phosphates released from radiolabeled Fizzy-pSer50 (Mochida et al., 2010). Addition of Arpp19

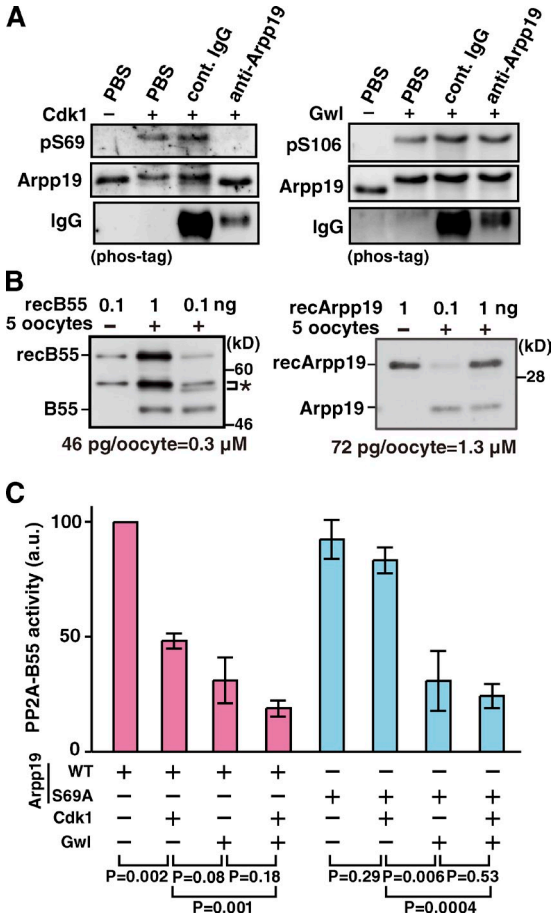

Figure 3. **Ser69 phosphorylation of Arpp19 by cyclin B–Cdk1 converts Arpp19 into an active inhibitor of PP2A-B55.** (A) Anti-Arpp19 antibody prevents in vitro phosphorylation on Ser69 of Arpp19 by cyclin B–Cdk1, but not on Ser106 by Gwl. Wild-type Arpp19 was preincubated with anti-Arpp19, control IgG, or PBS, and then phosphorylated with cyclin B–Cdk1 (left) or Gwl (right). Arpp19 phosphorylation was monitored by immunoblot with anti-pSer69 (left) or anti-pSer106 (right). (B) Estimation of the endogenous concentrations of B55 and Arpp19 proteins in starfish oocytes. Indicated amounts of recombinant GST-B55 (recB55; left) or recombinant Arpp19 (recArpp19; right) and/or five starfish oocytes were loaded and analyzed by Western blot. The concentrations of endogenous B55 (left) and Arpp19 (right) were calculated to be 0.3 and 1.3 μM, respectively, from protein amounts of 46 and 72 pg per 3 nl of oocyte volume. Asterisk, nonspecific bands. (C) Arpp19 phosphorylated in vitro on Ser69 by cyclin B–Cdk1 suppresses PP2A-B55 activity. Wild-type Arpp19 or the Ser69Ala (S69A) mutant protein was thiophosphorylated by cyclin B–Cdk1, Gwl, or both kinases, and then mixed with recombinant PP2A-B55 heterotrimers. Final concentrations of PP2A-B55 and Arpp19 in the mixture were adjusted to be 50 and 200 nM, respectively. After removal of kinases, phosphatase activity of PP2A-B55 was measured using Fizzy-pSer50 as a substrate. Each error bar indicates mean value ± SD from three independent experiments.

phosphorylated by cyclin B–Cdk1 alone reduced the PP2A-B55 activity to approximately half of controls with unphosphorylated Arpp19, whereas the phosphorylations by Gwl or by Gwl + cyclin B–Cdk1 were slightly or significantly more effective, respectively. The Ala mutant of Arpp19-Ser69, which had been treated with cyclin B–Cdk1, exhibited little reduction in PP2A-B55–inhibiting activity. These observations indicate that the Ser69 phosphorylation of Arpp19 by cyclin B–Cdk1 converts Arpp19 into a functional inhibitor against PP2A-B55, at least to some extent.

Our results collectively suggest that, in the absence of Gwl, the autoregulatory loop functions most likely through a novel bypass in which active cyclin B–Cdk1 directly phosphorylates Arpp19 on Ser69 to suppress PP2A-B55 (see Fig. 5). This model explains why Arpp19 is required for full activation of cyclin B–Cdk1 even when Gwl is not present. The implication would be that a partial reduction of PP2A-B55 activity is sufficient for the autoregulatory activation of cyclin B–Cdk1. In contrast, this is unlikely in frog egg extracts, where Gwl has been reported to be necessary for activation of cyclin B–Cdk1 (Yu et al., 2006). One interesting possible explanation for this discrepancy between organisms involves the unusual cytoplasmic localization of Gwl in frog oocytes (Hara et al., 2012).

Gwl phosphorylation of Arpp19 is required for chromosome segregation

Even though phosphorylation of Arpp19 on Ser106 by Gwl is not essential for the autoregulatory activation of cyclin B–Cdk1, this site (as well as Ser69) is indeed phosphorylated in vivo in M phase of starfish oocytes (see Figs. 1 B and 2 A). Does this phosphorylation on Ser106 by Gwl play some other critical role in M phase events? To address this question, we examined the behavior of meiotic chromosomes after GVBD in oocytes in which Gwl activation was prevented by injection with a neutralizing antibody against Gwl (Hara et al., 2012). We showed previously that after 1-MeAde is added to such oocytes, Gwl remains unactivated but cyclin B–Cdk1 is fully activated (Hara et al., 2012); hence, Arpp19 is assumed to be phosphorylated on Ser69 but not on Ser106. The Gwl-inhibited oocytes failed to segregate homologous chromosomes at the first polar body formation of meiosis I (Fig. 4, A and C). Further injection of Arpp19 that had been thiophosphorylated beforehand by Gwl on Ser106 restored the defect in chromosome segregation, whereas control injection of the wild-type Arpp19, which is assumed to have been phosphorylated on Ser69 but not on Ser106 within the oocytes, failed to show the restoration effect (Fig. 4, B and C). Thus the Gwl-dependent phosphorylation of Arpp19 on Ser106 is required for proper chromosome segregation. Chromosome segregation failure has also been observed in the Scant/Gwl mutant of *Drosophila melanogaster* (Yu et al., 2004; Archambault et al., 2007) and in human cells in which Gwl/MASTL has been knocked down (Burgess et al., 2010; Voets and Wolthuis, 2010). It is most likely that a partial reduction of PP2A-B55 activity effected by cyclin B–Cdk1 alone is not sufficient and its further reduction by cyclin B–Cdk1 plus Gwl is required to ensure proper chromosome segregation (Figs. 3 C and 5). In other words, the Gwl–Arpp19–PP2A-B55 pathway appears to exhibit more impact after nuclear envelope breakdown (Hara et al., 2012; Álvarez-Fernández et al., 2013; Cundell et al., 2013).

We show here that direct phosphorylation of Arpp19 on Ser69 by cyclin B–Cdk1 is sufficient for full activation of cyclin B–Cdk1 via its autoregulatory loop. The evolutionary implications of this finding are of interest. The homologous site for Ser69 of starfish Arpp19 is present in frog Ensa on Thr28, frog Arpp19 on Ser28, human Arpp19 on Ser23, and *C. elegans* Ensa on Ser21; but it is not present in human Ensa or the single Ensa family member in fruit flies (Fig. S1). We propose that Cdk1-dependent phosphorylation or a phosphomimetic mutation of at least one family member is required for mitotic progression in all metazoans. In fruit flies, the equivalent position to Ser69 is a phosphomimetic aspartic acid (Kim et al., 2012). In *C. elegans*, which appears not to have a Gwl homologue (Kim et al., 2012), Cdk1 phosphorylation of Ensa on Ser21 and other sites appears to compensate for the lack of Gwl phosphorylation.

Our results are most simply interpreted as indicating a biphasic regulation of the activity of Arpp19 in terms of its inhibition of PP2A-B55 (Fig. 5). In the initial stages, phosphorylation on Ser69 by a small population of activated cyclin B–Cdk1 plays a key role in the further autoactivation of larger pools of cyclin B–Cdk1. Activated cyclin B–Cdk1 can then activate Gwl, which then phosphorylates Ser106 on Arpp19, promoting synergistic autoactivation of cyclin B–Cdk1 and allowing proper segregation of chromosomes. These different roles of Arpp19 most likely reflect the types or levels of PP2A-B55 inhibition caused by the two phosphorylations. More plausibly, various substrates likely have different sensitivities to various levels of PP2A-B55 phosphatase activity: it will be intriguing to identify the substrates that exhibit the greater or least sensitivities to the inhibition of PP2A-B55 and determine whether a correlation exists with the different cellular roles of Arpp19 phosphorylated at the two sites.

Materials and methods

Starfish oocytes

Starfish *Asterina pectinifera* (renamed *Patiria pectinifera* in the 2007 National Center for Biotechnology Information Taxonomy Browser) were collected during the breeding season and kept in laboratory aquaria supplied with circulating seawater at 14°C. Fully grown immature oocytes without follicles were released from isolated ovaries after treatment with calcium-free artificial seawater (Ookata et al., 1992). These immature oocytes were treated with 1 µM 1-MeAde (Kanatani et al., 1969) to induce meiotic maturation at 20°C in artificial seawater. Microinjection and enucleation were performed as described previously (Kishimoto, 1986). Starfish oocytes were optically transparent, and hence an enucleated oocyte was easily prepared by suction of the whole germinal vesicle content and its membrane into a micropipette under microscopy. The use of all animals (starfish and rabbits) complied with our institute regulations.

cDNA cloning of starfish Arpp19 and B55

A cDNA clone covering the full-length starfish Arpp19 coding region was isolated by PCR, using first strand cDNA from poly(A) mRNA of immature starfish oocytes and specific primers designed from the 5′ and 3′ noncoding region of a gene (isotig11736; Human Genome Sequencing Center, Baylor College of Medicine) of another starfish species, *Asterina miniata*, that was homologous to *Xenopus laevis* Arpp19: 5′-AGTCTTCGCTCCAGCCACTCC-3′ forward and 5′-CATCCCCTTCCTCGCCCACT-3′ reverse. The PCR products were sequenced and confirmed to be homologous to Arpp19. The GenBank accession number for the cDNA sequence of the starfish *A. pectinifera* Arpp19 is AB818897. A cDNA of starfish 55-kD B subunit of PP2A (B55) was obtained from the starfish *A. pectinifera* expressed sequence tag cDNA library (clone ID apg14g01; GenBank accession no. AB818896).

Recombinant proteins

N-Terminal 6×His-tagged and C-terminal FLAG-tagged, full-length recombinant starfish Arpp19 protein was expressed in *Escherichia coli* BL21 (DE3; Invitrogen) using pET21b (EMD Millipore). Arpp19 protein was purified with Ni-NTA agarose (QIAGEN) and dialyzed against PBS (13.7 mM NaCl, 0.27 mM KCl, 0.75 mM Na_2HPO_4, and 0.15 mM KH_2PO_4). Ala mutants on putative phosphorylation sites of Arpp19 (T42A, S69A, S106A, and T155A) were generated with the QuikChange site-directed mutagenesis kit (Agilent Technologies). Primers for each mutation were as follow. T42A: forward, 5′-GAAGACAAGCCCGCCCCTCTGCCATTAC-3′;

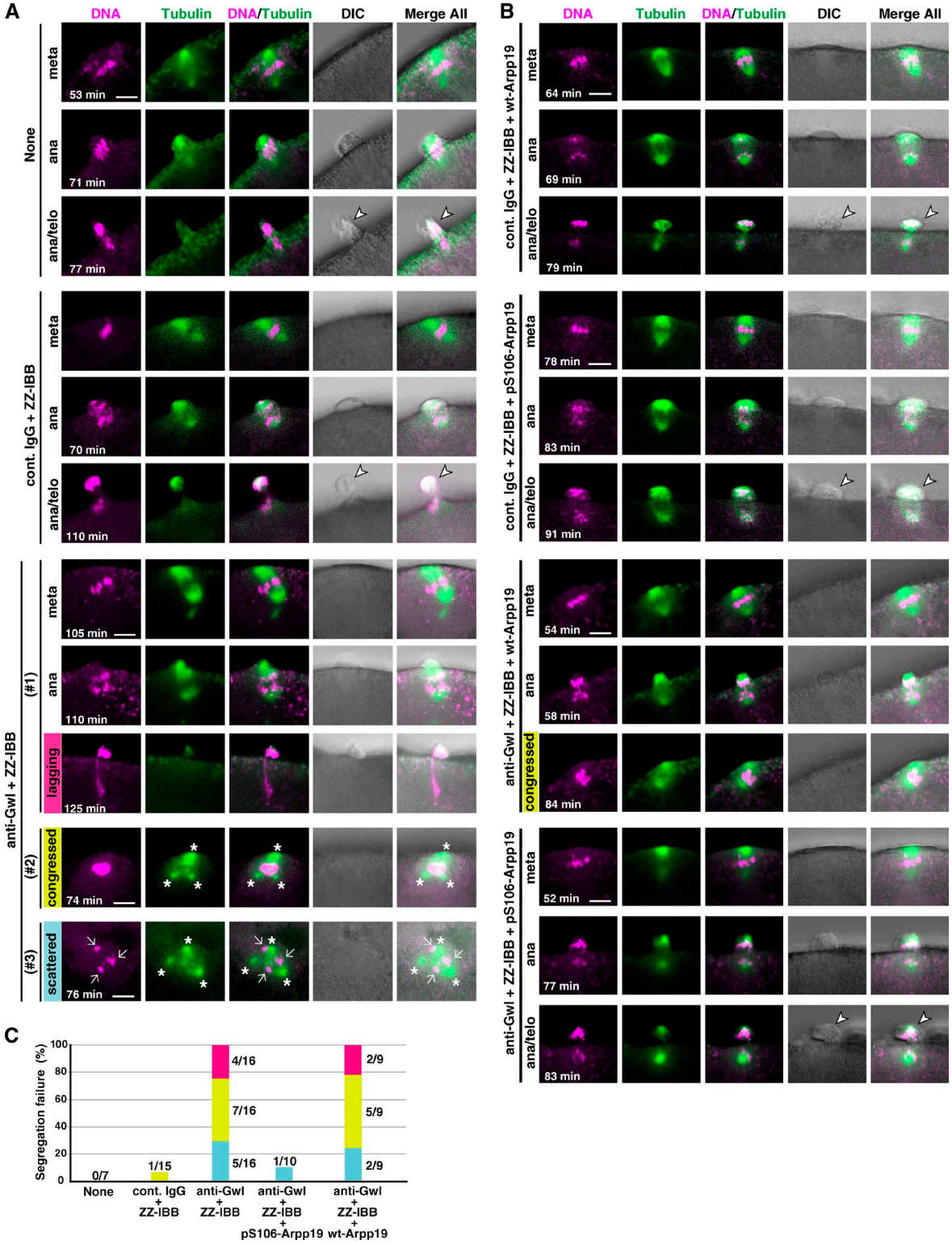

Figure 4. **Chromosome segregation in meiosis I is abortive in Gwl-inhibited oocytes.** (A and B) Immature starfish oocytes were first injected with HiLyte 488–labeled tubulin (green) and Alexa 568–labeled histone H1 (magenta), and then injected with neutralizing anti-Gwl antibody (anti-Gwl) or control IgG (cont. IgG) along with ZZ-IBB (that can deliver cytoplasmically injected IgG into the nucleus) or uninjected (None). After 1-MeAde addition, live-cell images were obtained using a confocal microscope to monitor formation of the meiosis I spindle. Gwl-inhibited oocytes failed to properly segregate homologous chromosomes (A). This phenotype may be classified into three types, although they overlapped in some cases: lagging (#1, magenta), congressed (#2, yellow), or scattered (#3, blue) chromosomes along with frequently multipolar spindles (asterisks). However, further coinjection into immature oocytes with Arpp19 that had been in vitro thiophosphorylated by Gwl (pS106-Arpp19), but not with wild-type Arpp19 (wt-Arpp19), restored homologous chromosome segregation (B). Time after 1-MeAde addition is indicated in each frame. Arrow, chromosomes; arrowhead, the first polar body. Bars, 5 µm. (C) Quantification of chromosome segregation failure displayed in A and B. Each color corresponds to #1, #2, and #3 in A and B, respectively. Numbers of independent experiments (more than three females) are indicated at each bar.

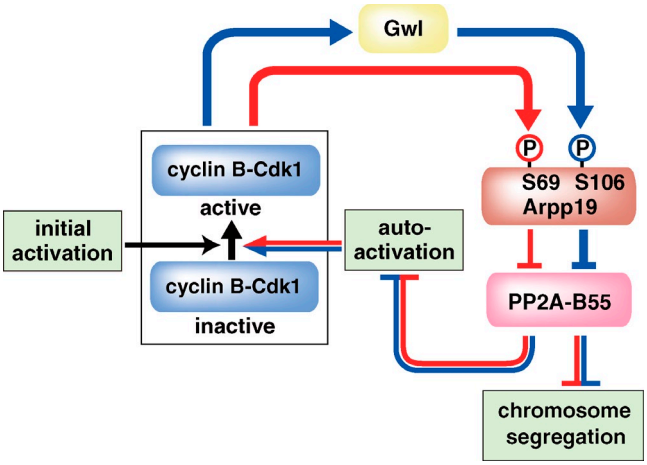

Figure 5. **Model for the two-step phosphorylation of Arpp19 and the distinct roles of the two phosphorylations in governing M phase.** First, phosphorylation on Ser69 by cyclin B–Cdk1 (red line) is involved in the autoregulatory activation of cyclin B–Cdk1. Second, further phosphorylation on Ser106 by Gwl (blue line) is needed for proper chromosome segregation, although it is not essential for the autoactivation. Initial activation corresponds to a trigger that reverses the balance between Cdc25 and Myt1/Wee1 before the first activation of cyclin B–Cdk1. Although molecular identity of the trigger remains elusive in most systems, it is clearly identified as Akt/PKB in the starfish oocyte (Okumura et al., 2002; Kishimoto, 2011): 1-MeAde causes activation of Akt/PKB, which in turn directly phosphorylates and inhibits Myt1 and phosphorylates and activates Cdc25, thus tipping the balance toward the initial activation of cyclin B–Cdk1.

reverse, 5′-GTAATGGCAGAGGGGCGGGCTTGTCTTC-3′; S69A: forward, 5′-GAAGCCTCAGCTCGCCCCTGAAAAGATG-3′; reverse, 5′-CATCTTTTCAGGGGCGAGCTGAGGCTTC-3′; S106A: forward, 5′-GTCAAATATTTTGACGCTGGGGATTACC-3′; reverse, 5′-GGTAATCCCCAGCGTCAAAATATTTGAC-3′; T155A: forward, 5′-GACCATCCCAGCCCCTGCCTCCATAC-3′; reverse, 5′-GTATGGAGGCAGGGGCTGGGATGGTC-3′. Multiple phosphorylation site mutants were generated with combinations of these primers. The PCR products were sequenced to confirm mutagenesis. Each mutant of Arpp19 protein was expressed, purified, and, after buffer exchange, concentrated at 4 mg/ml in PBS with Vivaspin 500–10 kD (Sartorius). These proteins were injected into oocytes at 0.3 ng/oocyte. His-tagged B55 protein and GST-tagged B55 protein were expressed in *E. coli*, and then purified with Ni-NTA agarose (QIAGEN) and glutathione Sepharose (GE Healthcare), respectively.

Preparation of active cyclin B–Cdk1 and active Gwl

Active cyclin B–Cdk1 was purified from meta-I starfish oocytes by Suc1 beads as described previously (Okumura et al., 1996). In brief, the high speed oocyte extracts (the supernatant after centrifugation at 140,000 *g* for 40 min) were first batch loaded on $p13^{Suc1}$–Sepharose 4B equilibrated with a buffer containing 80 mM β-glycerophosphate, 20 mM EGTA, 15 mM $MgCl_2$, 1 mM DTT, and 0.01% Brij35, pH 7.3. The Suc1 beads were then packed into a chromatographic column. After washing the column, starfish cyclin B–Cdk1 was eluted with the same buffer supplemented with 500 mM NaCl and 50% ethylene glycol. Purified cyclin B–Cdk1 fractions were dialyzed against a buffer containing 80 mM β-glycerophosphate, 20 mM EGTA, 15 mM $MgCl_2$, 1 mM DTT, 10% sucrose, and 0.1% NP-40, pH 7.3. N-Terminal 6×His-tagged, full-length recombinant Gwl proteins (active and inactive rGwl-WT, prepared in the presence or absence of okadaic acid, respectively, and kinase-deficient mutant) were prepared using the Bac-to-Bac Baculovirus expression system (Invitrogen) as described previously (Hara et al., 2012). In brief, 96 h after infection with recombinant baculovirus, Sf9 cells were lysed and rGwl was purified with Ni-NTA agarose. To prepare mitotically active rGwl-WT, Sf9 cells were treated with 100 nM okadaic acid for 12 h before harvest according to Yu et al. (2006). The kinase-deficient mutant of rGwl (rGwl-G52S) was generated with the QuikChange site-directed mutagenesis kit. Purified rGwl was dialyzed against a buffer containing 80 mM NaCl, 1 mM DTT, and 20 mM Hepes, pH 7.5.

In vitro phosphorylation of Arpp19

Wild-type and several mutant Arpp19 proteins were mixed with active cyclin B–Cdk1 and/or active Gwl in the presence of 1 mM ATP or 1 mM ATP-γ-S at 25°C for 60 min. Thiophosphorylated Arpp19 was separated from the kinases into the flow-through fraction using the centrifugal filter unit Ultrafree-MC (MW cutoff 30 kD; EMD Millipore), and after buffer exchange, concentrated with Vivaspin 500–10 kD to 1 mg/ml in TBS (50 mM Tris-HCl, pH7.5, and 150 mM NaCl) for phosphatase activity assay or in PBS for injection into oocytes.

In vivo phosphatase activity assay

Maltose-binding protein fused with 25 peptide residues containing Ser50 of Fizzy (Fizzy-Ser50) was expressed in *E. coli* and purified with amylose resin (New England Biolabs, Inc.; Mochida et al., 2009). 2 mg/ml of purified Fizzy-Ser50 was completely phosphorylated by starfish cyclin B–Cdk1 at 25°C for 2 h, and then repurified with amylose resin to remove kinase. Fizzy-pSer50 was injected into nucleated or enucleated oocytes (at 0.9 ng/oocyte) at the immature state, just after GVBD, or at a time equivalent to GVBD (enucleated oocytes). Oocytes were collected 15 min later and dissolved in Laemmli's sample buffer (LSB), and the phosphorylation state of Fizzy-Ser50 was analyzed by immunoblots with anti–maltose-binding protein antibody after phos-tag SDS-PAGE.

In vitro phosphatase activity assay

In vitro assay of phosphatase activity was performed using recombinant heterotrimeric PP2A-B55 complex (PP2A-A/B55δ/C) and its substrate, Fizzy-pSer50, as described previously (Mochida et al., 2010) with a small modification in assay conditions. Fizzy-Ser50 was phosphorylated by the purified starfish cyclin B–Cdk1 as described above in the presence of 1/50 volume of γ-[^{32}P]ATP (PerkinElmer), followed by removal of the kinase and unincorporated γ-[^{32}P]ATP with amylose resin. PP2A-B55 and Arpp19 were preincubated for 15 min on ice at the molar ratio 1:4 (final concentrations, 50 and 200 nM, respectively), which reflects the endogenous molar ratio in starfish oocytes. They were then supplemented with Fizzy-pSer50 (5,000 cpm), followed by phosphatase reaction for 30 min at 23°C. The reaction was terminated by adding 5 vol of 10% TCA. After protein precipitation by centrifugation, 15 µl of supernatant was mixed with 20 µl of 5% (wt/vol) ammonium molybdate in 0.5 M H_2SO_4 and 80 µl of water-saturated 2-methyl-1-propanol/heptane (1:1) to separate released phosphate as phosphomolybdic acid in alcohol. The radioactivity of the organic phase was counted with a liquid scintillation counter (LS6500; Beckman Coulter).

Gwl inhibition and its rescue

To inhibit the activity of nuclear Gwl in vivo, a neutralizing anti–Gwl-C antibody (3 mg/ml, 750 pg) was incubated with ZZ-IBB (10 mg/ml, 500 pg) for 30 min on ice, and then injected into the cytoplasm of immature oocytes as described previously (Hara et al., 2012). ZZ-IBB is composed of two synthetic Z domains derived from the IgG-binding domain of protein A and the nuclear localization signal IBB (importin β-binding domain of importin α), allowing nuclear accumulation of IgG (Hara et al., 2012). To examine whether Arpp19 restored the defect observed in Gwl-inhibited oocytes, either wild-type Arpp19 protein or Arpp19 protein that had been thiophosphorylated by Gwl (pS106-Arpp19; both 2 mg/ml) was microinjected into immature oocytes at sevenfold excess to the endogenous level, along with anti-Gwl antibody plus ZZ-IBB. Depending on batches of oocytes, coinjection of control IgG and ZZ-IBB caused some delay in reaching metaphase. Coinjection of anti-Gwl antibody caused further delay, whereas this additional delay was almost restored by further injection of pS106-Arpp19.

Live-cell images of microtubules and chromosomes

To monitor meiotic spindle assembly and chromosome alignment, each immature oocyte was injected with both 2% oocyte volume of HiLyte-488–labeled porcine brain tubulin (~2 mg/ml; Cytoskelton, Inc.) in G buffer (100 mM Pipes-KOH, pH 6.9, 1 mM $MgSO_4$, 1 mM EGTA, and 1 mM GTP) and with 1% oocyte volume of Alexa 568–labeled histone H1 in PBS (prepared at ~1 mg/ml using histone H1 protein [Roche] and Alexa 568 protein labeling kit [Molecular Probes]) as described previously (Hara et al., 2012). Live oocytes in artificial seawater were observed with a Fluoview FV1000 confocal microscope (Olympus) using a 40× water-immersion objective lens (UAPON 40×W340; Olympus) at 21°C. Fluoview software was used for acquisition of digital images from the photon detector of the FV1000 system. ImageJ software (National Institutes of Health) was used for Z-stack projection of maximum intensity, trimming, and adjustment of brightness and contrast of the obtained images. The levels of small-dotted noise signals

observed in oocytes injected with labeled histone H1 and labeled tubulin (see an original image in the DataViewer data) were reduced to the background level to easily distinguish chromosome signals. The processed images were exported as JPG files. Adobe Illustrator was used for the preparation of Fig. 4.

Antibodies

Three kinds of anti–starfish Arpp19 rabbit polyclonal antibodies were raised: anti-Arpp19 against recombinant full-length Arpp19 protein; anti–pS106-Arpp19 against KLH+C+KYFD(pS)GDYEM peptide (102–111 amino acid residues containing phospho-Ser106; Fig. S1), in which KLH (Keyhole limpet hemocyanin) was conjugated with sulfhydryl group at the additional N-terminal Cys; and anti–pS69-Arpp19 against KLH+CVKPQL(pS)PEKME (63–74 amino acid residues containing Cys63 and phospho-Ser69; Fig. S1). Each antibody was affinity purified with Immobilon membranes (EMD Millipore) to which recombinant protein was transferred as described previously (Okano-Uchida et al., 2003) or with peptide-conjugated Sulfo-link coupling resin (Thermo Fisher Scientific). Purified antibodies were concentrated with Vivaspin 2–50 kD, followed by buffer exchange to PBS. Concentrated anti-Arpp19 antibody (0.6 mg/ml) was used for injection into immature oocytes, for immunoprecipitation, and for inhibition of in vitro phosphorylation by cyclin B–Cdk1. The anti-pS106 and anti-pS69 antibodies were concentrated to 0.5 mg/ml and used for immunoblotting. To generate anti–starfish B55 antibody, a rabbit polyclonal antibody was raised against the His-tagged B55 protein and affinity purified with the GST-tagged B55 protein.

Immunoblots

Immunoblotting was performed as described previously (Okano-Uchida et al., 2003). Primary antibodies used were anti–starfish Myt1 (affinity-purified rabbit polyclonal antibody raised against N-terminal 124 amino acids [Okumura et al., 2002]; 1:500 in Can Get Signal Immunoreaction Enhancer [Can Get Signal] solution 1 [TOYOBO]), anti–starfish Cdc25 (affinity-purified rabbit polyclonal antibody raised against C-terminal 153 amino acids [Okumura et al., 1996]; 1:3,000 in Can Get Signal solution 1), anti–starfish cyclin B (affinity-purified rabbit polyclonal antibody raised against full-length cyclin B [Okano-Uchida et al., 1998]; 1:1,000 in Can Get Signal solution 1), anti-PSTAIR for Cdk1 (mouse monoclonal [Sigma-Aldrich]; 1:5,000 in TBS containing 0.1% Tween 20 [TBS-T]), anti–phospho-Cdk1 (rabbit polyclonal anti–phospho-Tyr15 [Cell Signaling Technology]; 1:500 in Can Get Signal solution 1), anti-MAPK (rabbit polyclonal [EMD Millipore]; 1:500 in TBS-T), anti-BM28 for Mcm2 (mouse monoclonal [BD]; 1:2,000 in TBS-T), anti–starfish Plk1 (affinity-purified rabbit polyclonal antibody raised against 30–431 amino acids [Okano-Uchida et al., 2003]; 1:200 in Can Get Signal solution 1), anti–starfish Gwl-C (affinity-purified rabbit polyclonal antibody raised against C-terminal 665–870 amino acids [Hara et al., 2012]; 1:1,000 in Can Get Signal solution 1), anti-B55 (described in Antibodies section; 1:500 in Can Get Signal solution 1), anti-Arpp19 (described in Antibodies section; 1:2,000 in Can Get Signal solution 1), anti–pS106-Arpp19 (described in Antibodies section; 1:500 in Can Get Signal solution 1), and anti–pS69-Arpp19 (described in Antibodies section; 1:100 in Can Get Signal solution 1). Because the anti–pS69-Arpp19 antibody did not have enough titer to detect phospho-Ser69 on Arpp19 in whole oocyte extracts, endogenous Arpp19 protein was first immunoprecipitated with anti-Arpp19 antibody, and then immunoblotted with anti-pSer69 antibody. Secondary antibodies were HRP-conjugated anti–rabbit IgG (donkey polyclonal [GE Healthcare]; 1:5,000 in TBS-T or Can Get Signal solution 2) or anti–mouse IgG (rabbit polyclonal [Dako]; 1:5,000 in TBS-T). Proteins reacting with the antibodies were detected with the ECL prime (GE Healthcare) and visualized with an imager (LAS4000; Fujifilm). To reprobe with another antibody, IgGs were stripped from the immunoblotted membranes by Stripping Solution as described in the ECL plus manual (GE Healthcare).

Immunoprecipitation

For immunoprecipitation of endogenous Arpp19 protein, anti-Arpp19 antibodies were bound and cross-linked with disuccinimidyl suberate to protein G–Sepharose (Sigma-Aldrich). Excess disuccinimidyl suberate was blocked by ethanolamine and beads were washed with TBS. About 50 µl of packed volume of starfish oocytes was collected after centrifugation at 5,000 *g* for 10 s at 4°C and frozen in liquid nitrogen. After thawing, the oocyte pellet was resuspended in 250 µl of a lysis buffer (80 mM β-glycerophosphate, 20 mM EGTA, 100 mM KCl, 15 mM $MgCl_2$, 100 mM sucrose, 1 mM DTT, 0.1% NP-40, and Complete EDTA-free [Roche], pH 7.3), left for 10 min on ice, and then lysed by vortex mixing in a cold room. After centrifugation at 12,000 *g* for 15 min at 4°C, the supernatant was recovered as an oocyte extract. For immunoprecipitation, 30 µl of the oocyte extract was incubated with 5 µl of anti-Arpp19 antibody beads for 90 min on ice. Each immunoprecipitate was washed three times with TBS-T, 15 µl of 2× LSB was added, and the samples were boiled for 5 min before electrophoresis.

SDS-PAGE and phos-tag SDS-PAGE

SDS-PAGE was performed as described previously (Okano-Uchida et al., 2003). To further separate phosphorylated proteins in SDS-PAGE, phos-tag acrylamide (Wako Chemicals USA) was added to the separation gel (10%, except for 12% in Fig. 3 A) at 22.5 µM with 45 µM $MnCl_2$, according to the manufacturer's instructions.

Histone H1 kinase assay

The activity of cyclin B–Cdk1 in oocytes was measured by in vitro phosphorylation of histone H1 as described previously (Okano-Uchida et al., 2003). 1 µl of oocytes extracts were incubated for 30 min at 25°C in a final volume of 10 µl containing 0.3 mg/ml histone H1 (Boehringer Ingelheim) and 0.2 µl of γ-[^{32}P]ATP. The reaction was terminated by addition of 10 µl of 2× LSB, followed by boiling for 5 min. 10-µl samples were run on 12% SDS-PAGE gel and stained with 0.25% Coomassie brilliant blue R-250. The gels were autoradiographed using an imaging plate with BAS2000 (Fujifilm).

Statistical analysis

Statistical analyses about averages, standard deviations, and two-tail p-values by paired *t* tests were performed using Microsoft Excel.

Online supplemental material

Fig. S1 shows deduced amino acid sequence of starfish Arpp19. Fig. S2 characterizes anti–starfish Arpp19, anti-pSer106 of Arpp19, anti-pSer69 of Arpp19, and anti–starfish B55 subunit of PP2A antibodies. Fig. S3 shows deduced amino acid sequence of starfish B55 regulatory subunit of PP2A. Online supplemental material is available at http://www.jcb.org/cgi/content/full/jcb.201307160/DC1. Additional data are available in the JCB DataViewer at http://dx.doi.org/10.1083/jcb.201307160.dv.

We thank Kazunori Tachibana, Daisaku Hiraoka, and Yusuke Abe for discussions and suggestions, and Michael L. Goldberg for critical reading of and invaluable suggestions on the manuscript.

M. Hara was supported by a postdoctoral fellowship from the Global Centers of Excellence program of the Japan Society for the Promotion of Science. This study was supported by grants-in-aid from the Ministry of Education, Science and Culture, Japan, to T. Kishimoto.

The authors declare no competing financial interests.

Submitted: 25 July 2013
Accepted: 24 January 2014

References

Abe, Y., E. Okumura, T. Hosoya, T. Hirota, and T. Kishimoto. 2010. A single starfish Aurora kinase performs the combined functions of Aurora-A and Aurora-B in human cells. *J. Cell Sci.* 123:3978–3988. http://dx.doi.org/10.1242/jcs.076315

Álvarez-Fernández, M., R. Sánchez-Martínez, B. Sanz-Castillo, P.P. Gan, M. Sanz-Flores, M. Trakala, M. Ruiz-Torres, T. Lorca, A. Castro, and M. Malumbres. 2013. Greatwall is essential to prevent mitotic collapse after nuclear envelope breakdown in mammals. *Proc. Natl. Acad. Sci. USA*. 110:17374–17379. http://dx.doi.org/10.1073/pnas.1310745110

Archambault, V., X. Zhao, H. White-Cooper, A.T.C. Carpenter, and D.M. Glover. 2007. Mutations in *Drosophila Greatwall/Scant* reveal its roles in mitosis and meiosis and interdependence with Polo kinase. *PLoS Genet.* 3:e200. http://dx.doi.org/10.1371/journal.pgen.0030200

Burgess, A., S. Vigneron, E. Brioudes, J.C. Labbé, T. Lorca, and A. Castro. 2010. Loss of human Greatwall results in G2 arrest and multiple mitotic defects due to deregulation of the cyclin B-Cdc2/PP2A balance. *Proc. Natl. Acad. Sci. USA*. 107:12564–12569. http://dx.doi.org/10.1073/pnas.0914191107

Castilho, P.V., B.C. Williams, S. Mochida, Y. Zhao, and M.L. Goldberg. 2009. The M phase kinase Greatwall (Gwl) promotes inactivation of PP2A/B55δ, a phosphatase directed against CDK phosphosites. *Mol. Biol. Cell*. 20:4777–4789. http://dx.doi.org/10.1091/mbc.E09-07-0643

Cundell, M.J., R.N. Bastos, T. Zhang, J. Holder, U. Gruneberg, B. Novak, and F.A. Barr. 2013. The BEG (PP2A-B55/ENSA/Greatwall) pathway ensures cytokinesis follows chromosome separation. *Mol. Cell*. 52:393–405. http://dx.doi.org/10.1016/j.molcel.2013.09.005

Ferrell, J.E., Jr., J.R. Pomerening, S.Y. Kim, N.B. Trunnell, W. Xiong, C.Y.F. Huang, and E.M. Machleder. 2009. Simple, realistic models of complex biological processes: positive feedback and bistability in a cell fate switch and a cell cycle oscillator. *FEBS Lett.* 583:3999–4005. http://dx.doi.org/10.1016/j.febslet.2009.10.068

Gharbi-Ayachi, A., J.C. Labbé, A. Burgess, S. Vigneron, J.M. Strub, E. Brioudes, A. Van-Dorsselaer, A. Castro, and T. Lorca. 2010. The substrate of Greatwall kinase, Arpp19, controls mitosis by inhibiting protein phosphatase 2A. *Science*. 330:1673–1677. http://dx.doi.org/10.1126/science.1197048

Hara, M., Y. Abe, T. Tanaka, T. Yamamoto, E. Okumura, and T. Kishimoto. 2012. Greatwall kinase and cyclin B-Cdk1 are both critical constituents of M-phase-promoting factor. *Nat. Commun.* 3:1059. http://dx.doi.org/10.1038/ncomms2062

Kanatani, H., H. Shirai, K. Nakanishi, and T. Kurokawa. 1969. Isolation and indentification on meiosis inducing substance in starfish *Asterias amurensis*. *Nature*. 221:273–274. http://dx.doi.org/10.1038/221273a0

Kim, M.Y., E. Bucciarelli, D.G. Morton, B.C. Williams, K. Blake-Hodek, C. Pellacani, J.R. Von Stetina, X. Hu, M.P. Somma, D. Drummond-Barbosa, and M.L. Goldberg. 2012. Bypassing the Greatwall–Endosulfine pathway: plasticity of a pivotal cell-cycle regulatory module in *Drosophila melanogaster* and *Caenorhabditis elegans*. *Genetics*. 191:1181–1197. http://dx.doi.org/10.1534/genetics.112.140574

Kishimoto, T. 1986. Microinjection and cytoplasmic transfer in starfish oocytes. *Methods Cell Biol.* 27:379–394. http://dx.doi.org/10.1016/S0091-679X(08)60359-3

Kishimoto, T. 2003. Cell-cycle control during meiotic maturation. *Curr. Opin. Cell Biol.* 15:654–663. http://dx.doi.org/10.1016/j.ceb.2003.10.010

Kishimoto, T. 2011. A primer on meiotic resumption in starfish oocytes: the proposed signaling pathway triggered by maturation-inducing hormone. *Mol. Reprod. Dev.* 78:704–707. http://dx.doi.org/10.1002/mrd.21343

Kishimoto, T., S. Hirai, and H. Kanatani. 1981. Role of germinal vesicle material in producing maturation-promoting factor in starfish oocyte. *Dev. Biol.* 81:177–181. http://dx.doi.org/10.1016/0012-1606(81)90360-2

Lew, D.J., and S. Kornbluth. 1996. Regulatory roles of cyclin dependent kinase phosphorylation in cell cycle control. *Curr. Opin. Cell Biol.* 8:795–804. http://dx.doi.org/10.1016/S0955-0674(96)80080-9

Lindqvist, A., V. Rodríguez-Bravo, and R.H. Medema. 2009. The decision to enter mitosis: feedback and redundancy in the mitotic entry network. *J. Cell Biol.* 185:193–202. http://dx.doi.org/10.1083/jcb.200812045

Lorca, T., C. Bernis, S. Vigneron, A. Burgess, E. Brioudes, J.C. Labbé, and A. Castro. 2010. Constant regulation of both the MPF amplification loop and the Greatwall-PP2A pathway is required for metaphase II arrest and correct entry into the first embryonic cell cycle. *J. Cell Sci.* 123:2281–2291. http://dx.doi.org/10.1242/jcs.064527

Mayer-Jaekel, R.E., H. Ohkura, P. Ferrigno, N. Andjelkovic, K. Shiomi, T. Uemura, D.M. Glover, and B.A. Hemmings. 1994. *Drosophila* mutants in the 55 kDa regulatory subunit of protein phosphatase 2A show strongly reduced ability to dephosphorylate substrates of p34cdc2. *J. Cell Sci.* 107:2609–2616.

Mochida, S., and T. Hunt. 2012. Protein phosphatases and their regulation in the control of mitosis. *EMBO Rep.* 13:197–203. http://dx.doi.org/10.1038/embor.2011.263

Mochida, S., S. Ikeo, J. Gannon, and T. Hunt. 2009. Regulated activity of PP2A-B55δ is crucial for controlling entry into and exit from mitosis in *Xenopus* egg extracts. *EMBO J.* 28:2777–2785. http://dx.doi.org/10.1038/emboj.2009.238

Mochida, S., S.L. Maslen, M. Skehel, and T. Hunt. 2010. Greatwall phosphorylates an inhibitor of protein phosphatase 2A that is essential for mitosis. *Science*. 330:1670–1673. http://dx.doi.org/10.1126/science.1195689

Nurse, P. 1990. Universal control mechanism regulating onset of M-phase. *Nature*. 344:503–508. http://dx.doi.org/10.1038/344503a0

Okano-Uchida, T., T. Sekiai, K. Lee, E. Okumura, K. Tachibana, and T. Kishimoto. 1998. *In vivo* regulation of cyclin A/Cdc2 and cyclin B/Cdc2 through meiotic and early cleavage cycles in starfish. *Dev. Biol.* 197:39–53. http://dx.doi.org/10.1006/dbio.1998.8881

Okano-Uchida, T., E. Okumura, M. Iwashita, H. Yoshida, K. Tachibana, and T. Kishimoto. 2003. Distinct regulators for Plk1 activation in starfish meiotic and early embryonic cycles. *EMBO J.* 22:5633–5642. http://dx.doi.org/10.1093/emboj/cdg535

Okumura, E., T. Sekiai, S. Hisanaga, K. Tachibana, and T. Kishimoto. 1996. Initial triggering of M-phase in starfish oocytes: a possible novel component of maturation-promoting factor besides cdc2 kinase. *J. Cell Biol.* 132:125–135. http://dx.doi.org/10.1083/jcb.132.1.125

Okumura, E., T. Fukuhara, H. Yoshida, S. Hanada, R. Kozutsumi, M. Mori, K. Tachibana, and T. Kishimoto. 2002. Akt inhibits Myt1 in the signalling pathway that leads to meiotic G2/M-phase transition. *Nat. Cell Biol.* 4:111–116. http://dx.doi.org/10.1038/ncb741

Ookata, K., S. Hisanaga, T. Okano, K. Tachibana, and T. Kishimoto. 1992. Relocation and distinct subcellular localization of p34cdc2-cyclin B complex at meiosis reinitiation in starfish oocytes. *EMBO J.* 11:1763–1772.

Rangone, H., E. Wegel, M.K. Gatt, E. Yeung, A. Flowers, J. Debski, M. Dadlez, V. Janssens, A.T.C. Carpenter, and D.M. Glover. 2011. Suppression of scant identifies Endos as a substrate of greatwall kinase and a negative regulator of protein phosphatase 2A in mitosis. *PLoS Genet.* 7:e1002225. http://dx.doi.org/10.1371/journal.pgen.1002225

Santos, S.D., R. Wollman, T. Meyer, and J.E. Ferrell Jr. 2012. Spatial positive feedback at the onset of mitosis. *Cell.* 149:1500–1513. http://dx.doi.org/10.1016/j.cell.2012.05.028

Vigneron, S., E. Brioudes, A. Burgess, J.C. Labbé, T. Lorca, and A. Castro. 2009. Greatwall maintains mitosis through regulation of PP2A. *EMBO J.* 28:2786–2793. http://dx.doi.org/10.1038/emboj.2009.228

Voets, E., and R.M.F. Wolthuis. 2010. MASTL is the human orthologue of Greatwall kinase that facilitates mitotic entry, anaphase and cytokinesis. *Cell Cycle*. 9:3591–3601. http://dx.doi.org/10.4161/cc.9.17.12832

Yu, J., S.L. Fleming, B. Williams, E.V. Williams, Z. Li, P. Somma, C.L. Rieder, and M.L. Goldberg. 2004. Greatwall kinase: a nuclear protein required for proper chromosome condensation and mitotic progression in *Drosophila*. *J. Cell Biol.* 164:487–492. http://dx.doi.org/10.1083/jcb.200310059

Yu, J., Y. Zhao, Z. Li, S. Galas, and M.L. Goldberg. 2006. Greatwall kinase participates in the Cdc2 autoregulatory loop in *Xenopus* egg extracts. *Mol. Cell*. 22:83–91. http://dx.doi.org/10.1016/j.molcel.2006.02.022

Zhao, Y., O. Haccard, R. Wang, J. Yu, J. Kuang, C. Jessus, and M.L. Goldberg. 2008. Roles of Greatwall kinase in the regulation of cdc25 phosphatase. *Mol. Biol. Cell*. 19:1317–1327. http://dx.doi.org/10.1091/mbc.E07-11-1099